An Open-Source Plate Reader

Karol Szymula[†], **Michael S. Magaraci**[†], **Michael Patterson**, **Andrew Clark**, **Sevile G. Mannickarottu**, **Brian Y. Chow**[*]

Department of Bioengineering, University of Pennsylvania, 210 South 33rd Street, Philadelphia, PA 19104.

Abstract

Microplate readers are foundational instruments in experimental biology and bioengineering that enable multiplexed spectrophotometric measurements. To enhance their accessibility, we here report the design, construction, validation, and benchmarking of an open-source microplate reader. The system features full-spectrum absorbance and fluorescence emission detection, in situ optogenetic stimulation, and stand-alone touch screen programming of automated assay protocols. The total system costs <$3500, a fraction of the cost of commercial plate readers, and can detect the fluorescence of common dyes down to ~10 nanomolar concentration. Functional capabilities were demonstrated in context of synthetic biology, optogenetics, and photosensory biology: by steady-state measurements of ligand-induced reporter gene expression in a model of bacterial quorum sensing, and by flavin photocycling kinetic measurements of a LOV (light-oxygen-voltage) domain photoreceptor used for optogenetic transcriptional activation. Fully detailed guides for assembling the device and automating it using the custom Python-based API (Application Program Interface) are provided. This work contributes a key technology to the growing community-wide infrastructure of open-source biology-focused hardware, whose creation is facilitated by rapid prototyping capabilities and low-cost electronics, opto-electronics, and microcomputers.

The creation of open-source hardware for enabling molecular and cellular studies is facilitated by the ready availability of rapid prototyping techniques, low-cost opto-

electronics, and commoditized microcomputers & micro-controllers. Such open-source platforms – which to date include fluorescence imagers[1, 2], spectrophotometers[3], turbidostats[4], robotic liquid handlers[5, 6], and multi-well plate illuminators for optogenetic stimulation[7, 8] – increase access to both standard and custom laboratory apparatus alike. Here, we report the creation of an open-source plate reader (OSP), which is one of the most ubiquitous and important technologies in experimental biochemistry, biology, and bioengineering, because a plate reader permits automated and multiplexed spectrophotometric measurements.

Plate readers typically consist of a multi-mode (absorbance / optical density, and fluorescence) spectrophotometer, plus a programmable-motion stage for multiplexing by serial positioning of sample wells of the plate over a single detector. Detection wavelengths are selected using diffraction gratings or dichroic filters, and excitation wavelengths are selected similarly or by using monochromatic or narrow-band excitation sources such as lasers and light-emitting diodes (LEDs). They may possess auxiliary input ports for fluid delivery, and these ports have been successfully co-opted for other purposes such as optogenetic stimulation[9]. However, commercial plate readers cost tens of thousands of $USD, which can be prohibitive for resource-limited environments including educational settings.

The open-source framework (Figure 1) reported here is intended to provide the necessary and modular functionalities of a commercial system, while maintaining the performance required for most assays at a fractional cost (<$3500 or ~10x reduction). The system features full visible spectrum absorbance and fluorescence emission capabilities, *in situ* optogenetic stimulation, and stand-alone touch screen programming of automated assay protocols. It is expandable and customizable, with built-in access- and communication ports for external modules to enhance function and its own Python-based Application Programming Interface (API). We document the design considerations, overview of system assembly and operation, benchmarking with standard fluorochrome dyes, and validation in molecular and cellular-level experiments in synthetic biology, optogenetics, and photobiology contexts.

RESULTS AND DISCUSSION

Opto-mechanical platform design.

The fundamental core of a plate reader is two-axis motion for x-y positioning with respect to a single set of fiber optic input/outputs, which enables multiplexing. Thus, we designed low-cost hardware and software frameworks (Figures 1 and 2) for automated motion, and for interfacing with open-source devices and fiber-coupled opto-electronics. For baseline functionality useful in most laboratory contexts, the open-source plate reader (OSP) employs a CCD (charge-coupled device) linear array detector with open-source drivers (Ocean Optics), and inexpensive dome-capped light-emitting diodes (LEDs) as illumination sources for absorbance / optical density (OD) measurements and for fluorescence measurements with common fluorochromes (Figure 1a). The use of fiber optics to couple the optical elements to the sampling location allows for modular choice in excitation sources and detectors, and importantly, also supports the expansion or customization through these

optical fibers to more sensitive detectors or to sources of higher power or different wavelengths. Thus, the system is designed as both a low-cost and expandable plate reader chassis.

For automated motion, a custom 3D-printed plate holder is attached to low-cost linear drive motors that provide positional feedback voltage readings. The motors were chosen to ensure sufficient travel range (140 mm) for plate loading and load-bearing capacity (100 N) for the plate stage. The motor-connected stage glides on a modular frame of extruded t-slotted aluminum, which was chosen for its ease of assembly and utility of the t-slot tracks themselves for alignment, similar to dovetail rails (Figure 1b). Plates are tightly and repeatably positioned into one corner of the holder by spring-loading, and loaded through a front door (Figure 1c).

For optical detection, an optomechanical lens cage assembly under the plate holds a collimating aspheric lens to couple transmitted and emitted (bottom fluorescence) light to a multi-mode fiber optic cable (Figure 1a, *left*). This patch cord can be connected to any fiber-compatible detector with a SMA fitting. In the baseline low-cost version here, we use a CCD-based Ocean Optics visible-range detector because of its available open-source drivers and overall balance of sensitivity, full-spectrum- and monochromatic detection, and relative low-cost compared to monochromator-coupled photomultiplier tubes (PMT).

For bottom fluorescence excitation, a 3D-printed component surrounds the detector fiber input assembly, and projects multiple light-sources onto the plate bottom. Three positions hold sockets connectors for dome-capped LEDs as cost-effective, bright, and built-in fluorescence excitation sources. Initially, these LEDs are blue, green, and orange (λ = 470 nm, 525 nm, and 610 nm) for exciting common dyes and fluorescent proteins, but they can be simply replaced with different standard dome-capped LEDs. In lieu of using collimating lenses, the LEDs have narrow solid angles which, combined with the acceptance angle of the collection aspheric, prevents well-to-well crosstalk. These LEDs can also be used for optogenetic stimulation. The OSP was designed for visible spectrum measurements of most plate reader assays, and thus similar to any commercial filter-based plate reader, omits a fully tunable excitation source like a scanning monochromator for fluorescence excitation scans.

An additional position of the projection assembly holds a SMA-terminated collimated fiber optic for use with external sources as alternatives or upgrades to dome-capped LEDs. For cases where the user requires multiple external sources coupled to the one collimated projection fiber, we suggest commercially available bifurcated or fan-out optical fibers (e.g. from Thorlabs) as a cost-effective alternative to traditional dichroic beam combiners, because the fiber-based solution is effectively universal by eliminating the minimum spectral separation for co-aligning optical sources with dichroic mirrors. However, such combiners are not recommended for co-aligning a detection fiber with excitation sources (i.e. 90° incident angle between sample and excitation), because direct back reflection from a collimating lens or plate bottom saturates the detector in the absence of an automated dichroic filter wheel or tunable diffraction gratings.

For top-side excitation for absorbance / optical density measurements and optogenetic stimulation, another optomechanical lens train (Figure 1a, ***right***) over the plate positions a visible-spectrum white light source, consisting of two LEDs (LED 1: λ = 430 – 660 nm, LED2: λ = 430 nm) (Figure S1). A laser-cut component connected to the top optical train positions an auxiliary port for external functionality like fluid delivery and optogenetic stimulation. Similar to commercial systems, the auxiliary port is offset from the detector with a ~5 sec delay between delivery of fluid/photons to the well and measurement from the well, although simultaneous of zero-delay optogenetic stimulation is possible using the bottom excitation sources. The auxiliary port is designed to couple to a standard optical lens cage plate for attaching and aligning custom components, which can be fed into the OSP through a grommet on top.

Automation and Interface Design.

The OSP can be operated by an external computer or Raspberry Pi microcomputer by using automated scripts or a Graphical User Interface (GUI) that supports touchscreen control (Figure 2). The GUI and automation software are programmed in Python. The description of the interface will assume the use of a Raspberry Pi from hereon for simplicity.

The Raspberry Pi / computer communicates directly with the detector to set acquisition parameters, and also sends programming commands to an Arduino microcontroller (Figure S2 and Supporting Note 1). The Arduino controls the other functions (LEDs, motors, and auxiliary functions) and synchronizes them with the detector data acquisition through digital logic. LED timing is controlled by digital switching of a transistor-gated current source. The motors are controlled by pulse width modulation commands sent to the commercial motor driver-boards, which also relay positional feedback (potentiometer readings). Auxiliary functions can be triggered by standard digital logic control of external devices. The Arduino serves as the input/output hub because the Raspberry Pi lacks general purpose analog inputs for positional feedback from the motors and alignment photodiode, without the use of a data acquisition device (DAQ) for analog-to-digital conversion. Furthermore, the instrument control architecture is preserved if another type of computer is substituted for the Raspberry Pi microcomputer.

The GUI (Supporting Note 1) emulates the basic programming capabilities of commercial plate readers. Acquisition parameters include: (i) detector integration time, (ii) selected data range for spectra (scan averaging, boxcar, excitation wavelength), (iii) time-step for kinetic acquisition, (iv) well selection and control (ordering, calibration (Figure S3)), and (v) coordination with auxiliary functions. Data spreadsheets are exported to local storage and can be manipulated locally in the Raspberry Pi environment using the open-source office software suite, LibreOffice (or similar).

Protocols: Device Construction and Operation.

Detailed step-by-step assembly guides and programming overview are available (Supporting Notes 1–4), as summarized here. Supporting Note 1 describes software installation, the organization of the open-source API, the available functions for custom programming, and a walk-through of the GUI operation. Supporting Note 2 provides assembly instructions for

the top and bottom optical trains shown in Figure 1a. Supporting Note 3 describes the assembly of the printed circuit boards and the photodiode assembly used for calibrating the spatial coordinates of the motor. Supporting Note 4 provides overall assembly instructions of the t-slotted frame, all custom 3D-printed or laser cut components including the plate stage (Supporting File 1), and the integration of all sub-components (trains, circuit boards, stage, and frame) into a complete device. The total cost of the system is <$3,500 (Table S1).

The use of lens cage assemblies allows for facile alignment of all optical components along the detection axis (Supporting Note 3). To initialize the spatial coordinates of the microplate wells post-assembly (Figure S3), transmission measurements are made through a mask overlaid on the plate, as detected by a fast photodiode (Figure 1b); an automated script identifies the center of three alignment wells and the plate edges to define the spatial map. This calibration protocol takes ~3 minutes, which is short enough to regularly perform to ensure repeatability.

An .iso file for software installation is available via a permanent link at the University of Pennsylvania's Scholarly Commons, where all necessary guides, schematics, software, and CAD files will be updated with version improvements; the site content of this site is mirrored at the GitHub software repository. CAD files and assembly guides are also available on the MetaFluidics CAD repository. The links can be found in Associated Content.

The 3D-printed parts were made from PLA (polylactic acid) filament, the most common material for desktop 3D-printers. Most 3D-printable polymers would be suitable unless they are water soluble in the event a spill (e.g. PVA (polyvinyl alcohol)), or they are soft (e.g. low-density polyethylene (LDPE)) or flexible materials (e.g. rubberized "flexible filament") materials that hold poorly over time when fastened under compression. Alternatively, the plate holder can be milled from metals and machinable rigid plastics like Delrin (polyoxymethylene). Laser cut parts were made from acrylic sheet, which is suitably stiff for fastening under compression and for remaining flat as a supported wall/floor (as is Delrin). Alternatively, the two-dimensional components can be machined from other hard sheets like metal, Lexan (polycarbonate), or PVC (polyvinylchloride), although these materials are incompatible with a CO_2-laser cutter. Wood-based materials are unsuitable for any component that requires dimensional stability because they swell with moisture.

Performance Benchmarking with Reference Dyes.

The baseline system performance was assessed using a reference standard fluorescent dye kit (Figure 3). The respective absorbance/emission peak spectra and extinction coefficients of the dyes were in line with expected values. Thus, the custom opto-mechanical elements do not introduce major aberrations. The fluorescence of NIST-traceable fluorescein could be measured with a ~10 nM limit of detection with the low-cost detector. Such a detection limit is sufficient for common fluorescence assays as intended, albeit greater than the ~10 pM limit of commercial systems that use PMTs.

The spectral separation required between fluorescence excitation and emission detection starting-wavelength was approximately one FWHM (full-width at half-maximum) of an

LED because of the collection of reflected light from the plate bottom (Figure S4). Given a typical ~30nm FWHM of dome-capped LEDs here, the separation is on par with the recommended separation of a commercial plate reader. The separation can be decreased as low-cost LEDs with narrower bandwidths become available, or with laser diodes.

The coefficient of variations across entire 24-well or 96-well plates were 1.9% and 3.1%, respectively, with maximum variation from the mean of 2.8% and 8.6%, respectively. The variability is largely set by the motor resolution (vs. that of high-precision stepper motors that are ~50-fold more expensive). The precision is sufficient for these common 24-well and 96-well plate formats, albeit unlikely for higher density 384-well plates and beyond.

The OSP acquires a full spectrum in ~11 sec per well (inclusive of the movement to the well). Because the CCD detector captures all wavelengths simultaneously, the acquisition time for a full spectrum is the same as a single wavelength measurement. While a commercial plate reader with a PMT detects single wavelengths in roughly the same time, the latter is much slower when measuring full spectra because it sweeps individual wavelengths; as a matter of reference, in our hands a Tecan microplate reader takes nearly six minutes to acquire a spectrum (400 nm-wide range with 2 nm step-size). This difference in time can be meaningful with samples in organic solvents prone to evaporation, or samples prone to sedimentation.

Validation in Cellular and Biomolecular Contexts.

We performed cellular and protein-level assays to demonstrate the standard and non-standard measurement functionalities of the OSP in biomolecular contexts. First, we measured the input/output transfer functions of bacterial "Receiver" strains[1, 10], where a fluorescent protein reporter expression is placed under the switch-like transcriptional regulation of the (acyl-homoserine-lactone) AHL-responsive *luxR* activator (Figure 4). This system was chosen for its widespread use in synthetic biology to systematically study transcriptional regulation and inter-cellular communication[10, 11], and also because it involves the two major functionalities of a plate reader of transmission measurements (optical density, absorbance) and fluorescence measurements needed to determine OD-normalized cellular fluorescence. The two *E. coli* strains differ by the presence or absence of an LVA degradation tag[12, 13] on the GFP reporter. The relative switching behaviors of these strains are consistent with our previously reported measurements on a commercial (Tecan) plate reader (see BC-A1–001 and BC-A1–002 in Supplement of Reference:[1]) with respect to half-saturation concentration of AHL and the relative magnitudes of GFP expression.

Next, we measured the flavin photocycling[14] kinetics of the light-oxygen-voltage domain (LOV) photoreceptor EL222 from purified recombinant protein[15]. This kinetic measurement (absorbance at 450nm, A450) monitors the blue light-induced formation and thermal reversion (in the dark) of a cysteinyl-flavin photoadduct that underlies photosensory signaling by LOV proteins, which are of great importance in photobiology and pervasive in use in optogenetics and synthetic biology[16, 17]. EL222 in particular is commonly studied to explore the structure-function of light-induced homodimerization, and the bacterial LOV is useful for light-activated transcriptional activation with high on/off contrast ratios in eukaryotes[18, 19]. The photocycling measurement (Figure 5) demonstrates the ability to

measure a kinetic time-course and coordinate the measurement with a programmed set of events, in this case, *in situ* optogenetic stimulation of an individual well. To date, such *in situ* illumination for multiplexed measurements requires custom modification of a commercial plate reader[9].

In summary, we report the design, construction, and validation of an open-source plate reader framework. The cost-effectiveness of the OSP highlights the importance to laboratory research of rapid prototyping technologies, low-cost solid-state opto-electronics, and minimal single-board micro-computers and micro-controllers. The open-source nature and modularity of the system will facilitate future customization or enhancements that incorporate improved components as they decrease in cost, such as high-power collimated LEDs and the use of metal 3D-printing. The low-cost, modular, and expandable plate reader will enhance access to, and flexibility of, a core instrument across biological and chemical disciplines.

ASSOCIATED CONTENT

Materials and Methods.

The parts list (including raw materials and vendors), step-by-step guides for hardware construction and calibration, and software installation and application programming can be found in Supporting Information, as described in "Protocols: Device Construction and Operation."

Circuit boards were printed by Advanced Circuits. T-slotted aluminum was cut to specification by 8020, Inc. Custom mechanical components were designed in Solidworks and fabricated at the George H. Stephenson Bioengineering Education Laboratory at the University of Pennsylvania. Laser cut parts were made on a Universal Laser Systems VLS 3.50 with acrylic sheets. 3D-printed parts were made on a MakerBot Replicator (5th Generation) with polylactic acid (PLA) filament. Custom mechanical components can be produced at a facility with similar equipment for rapid prototyping or CNC-machining (mill and waterjet cutting), such as a local/university machine shop or commercial service (e.g. eMachineShop).

All assays were cross-validated on a commercial Tecan Infinite M200 plate reader. The volume-dependent effective path length in 24-well plates was calculated from Beer's Law plots of NIST-traceable fluorescein (F36915, NIST Standard Reference Material 1932[20]) at A(490 nm) assuming ε = 87,000 M-1 cm-1 [Conversion factor: 2.18 mL fluid ~ 1 cm effective pathlength, linear down to 500 μL volume]. Reference dye measurements were performed according to kit manufacturer protocols (Thermo Fisher R14782), using an integration period of 1.25 seconds. Quorum sensing experiments were performed as described previously[1]. Recombinant EL222 was bacterially produced and FPLC-purified as described previously[21]. Fluorescence detection limit was measured by reported methods for determining plate reader sensitivity[22], with 0.3 μM NIST-traceable fluorescein and an integration time of 1.25 seconds.

Supplementary Material

Refer to Web version on PubMed Central for supplementary material.

ACKNOWLEDGMENT

REFERENCES

[1]. Magaraci MS, Bermudez JG, Yogish D, Pak DH, Mollov V, Tycko J, Issadore D, Mannickarottu SG, and Chow BY (2016) Toolbox for Exploring Modular Gene Regulation in Synthetic Biology Training, ACS synthetic biology 5, 781–785. [PubMed: 27111289]

[2]. Nuñez I, Matute T, Herrera R, Keymer J, Marzullo T, Rudge T, and Federici F (2017) Low cost and open source multi-fluorescence imaging system for teaching and research in biology and bioengineering, PLOS ONE 12, e0187163. [PubMed: 29140977]

[3]. Albert DR, Todt MA, and Davis HF (2012) A Low-Cost Quantitative Absorption Spectrophotometer, Journal of Chemical Education 89, 1432–1435.

[4]. Takahashi CN, Miller AW, Ekness F, Dunham MJ, and Klavins E (2015) A Low Cost, Customizable Turbidostat for Use in Synthetic Circuit Characterization, ACS synthetic biology 4, 32–38. [PubMed: 25036317]

[5]. Gerber LC, Calasanz-Kaiser A, Hyman L, Voitiuk K, Patil U, and Riedel-Kruse IH (2017) Liquid-handling Lego robots and experiments for STEM education and research, PLOS Biology 15, e2001413. [PubMed: 28323828]

[6]. Steffens S, Nüßer L, Seiler T-B, Ruchter N, Schumann M, Döring R, Cofalla C, Ostfeld A, Salomons E, Schüttrumpf H, Hollert H, and Brinkmann M (2017) A versatile and low-cost open source pipetting robot for automation of toxicological and ecotoxicological bioassays, PLOS ONE 12, e0179636. [PubMed: 28622373]

[7]. Gerhardt KP, Olson EJ, Castillo-Hair SM, Hartsough LA, Landry BP, Ekness F, Yokoo R, Gomez EJ, Ramakrishnan P, Suh J, Savage DF, and Tabor JJ (2016) An open-hardware platform for optogenetics and photobiology, Scientific Reports 6, 35363. [PubMed: 27805047]

[8]. Hannanta-Anan P, and Chow BY (2016) Optogenetic Control of Calcium Oscillation Waveform Defines NFAT as an Integrator of Calcium Load, Cell systems 2, 283–288. [PubMed: 27135540]

[9]. Richter F, Scheib US, Mehlhorn J, Schubert R, Wietek J, Gernetzki O, Hegemann P, Mathes T, and Moglich A (2015) Upgrading a microplate reader for photobiology and all-optical experiments, Photochem. Photobiol. Sci 14, 270–279. [PubMed: 25373866]

[10]. Basu S, Gerchman Y, Collins CH, Arnold FH, and Weiss R (2005) A synthetic multicellular system for programmed pattern formation, Nature 434, 1130–1134. [PubMed: 15858574]

[11]. Gerchman Y, and Weiss R (2004) Teaching bacteria a new language, Proceedings of the National Academy of Sciences of the United States of America 101, 2221–2222. [PubMed: 14982990]

[12]. Farrell CM, Grossman AD, and Sauer RT (2005) Cytoplasmic degradation of ssrA-tagged proteins, Molecular Microbiology 57, 1750–1761. [PubMed: 16135238]

[13]. Purcell O, Grierson CS, Bernardo M. d., and Savery NJ (2012) Temperature dependence of ssrA-tag mediated protein degradation, Journal of Biological Engineering 6, 10–10. [PubMed: 22824000]

[14]. Zayner JP, and Sosnick TR (2014) Factors That Control the Chemistry of the LOV Domain Photocycle, PLOS ONE 9, e87074. [PubMed: 24475227]

[15]. Nash AI, McNulty R, Shillito ME, Swartz TE, Bogomolni R. a., Luecke H, and Gardner KH (2011) Structural basis of photosensitivity in a bacterial light-oxygen-voltage/helix-turn-helix (LOV-HTH) DNA-binding protein, Proceedings of the National Academy of Sciences of the United States of America 108, 9449–9454. [PubMed: 21606338]

[16]. Christie JM, Gawthorne J, Young G, Fraser NJ, and Roe AJ (2012) LOV to BLUF: flavoprotein contributions to the optogenetic toolkit, Mol Plant 5, 533–544. [PubMed: 22431563]

[17]. Pudasaini A, El-Arab KK, and Zoltowski BD (2015) LOV-based optogenetic devices: light-driven modules to impart photoregulated control of cellular signaling, Frontiers in molecular biosciences 2, 18. [PubMed: 25988185]

[18]. Motta-Mena LB, Reade A, Mallory MJ, Glantz S, Weiner OD, Lynch KW, and Gardner KH (2014) An optogenetic gene expression system with rapid activation and deactivation kinetics, Nat Chem Biol 10, 196–202. [PubMed: 24413462]

[19]. Reade A, Motta-Mena LB, Gardner KH, Stainier DY, Weiner OD, and Woo S (2017) TAEL: a zebrafish-optimized optogenetic gene expression system with fine spatial and temporal control, Development 144, 345–355. [PubMed: 27993986]

[20]. (2017) Fluorescein, Certificate of Analysis, Standard Reference Material 1932, National Institute of Standards and Technology, Gaithersburg, MD.

[21]. Glantz ST, Berlew EE, Jaber Z, Schuster BS, Gardner KH, and Chow BY (2018) Directly light-regulated binding of RGS-LOV photoreceptors to anionic membrane phospholipids, Proceedings of the National Academy of Sciences 115, E7720–E7727.

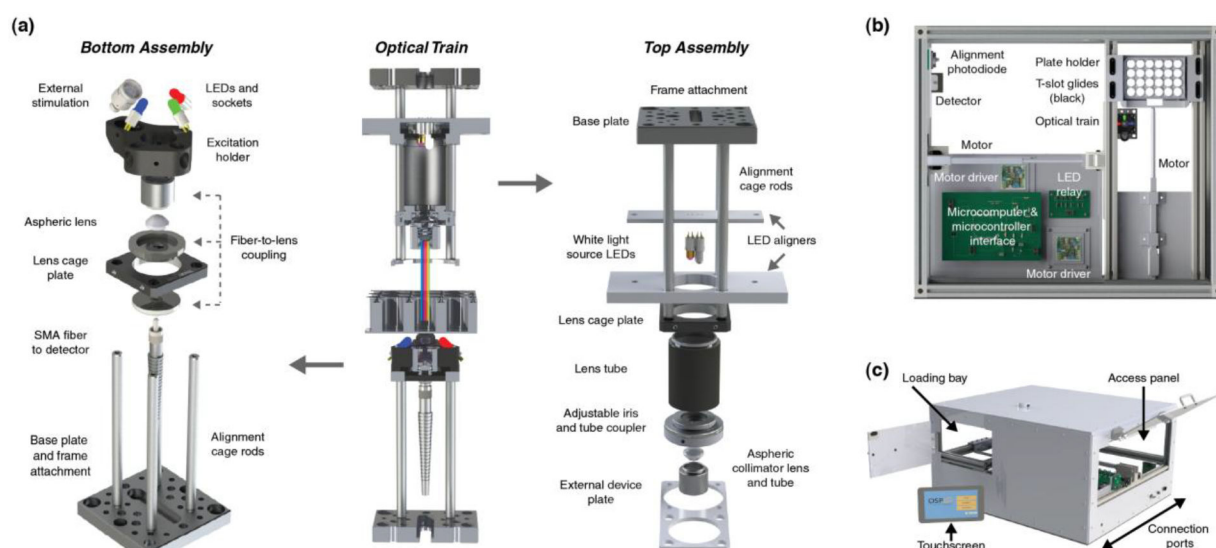[22]. (2010) Techninal Note – Inifinite Pro FI Bottom Sensitivity, Tecan Group Limited, Männedorf, Switzerland.

Figure 1. Opto-mechanical summary of the open-source plate reader (OSP).
All images are CAD renderings. **(a)** The optical train, with exploded views of bottom assembly for detection and optical excitation, and the top assembly for the white light source for optical density measurements and for external devices (e.g. high-power optogenetic stimulation or fluid delivery). The white light source combines two LEDs to span the visible spectrum. **(b)** Top-down view of the whole instrument. The relay board contains header blocks that consolidate connections of the individual device components, separated from the main microcomputer board. The top optical train is omitted for clarity. **(c)** Isometric view of the instrument, with touchscreen that can be mounted. All connections and access for repair are consolidated on one side.
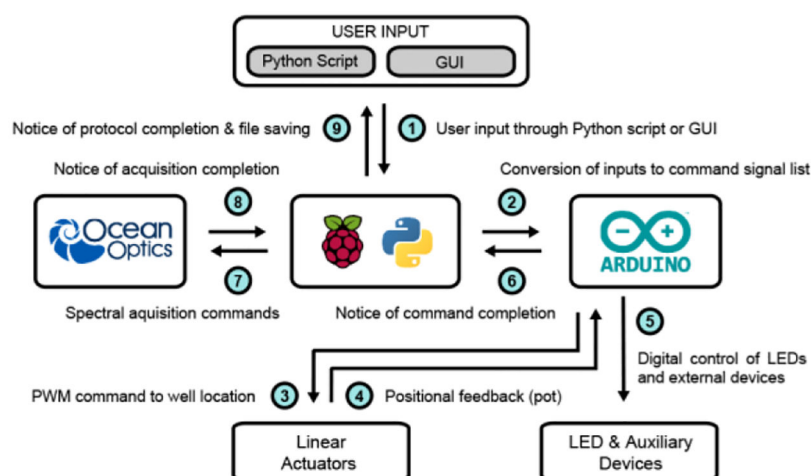
Figure 2. Device integration and automation workflow.
User inputs to a Raspberry Pi microcomputer (center) are entered via the graphical user interface (GUI) or written Python script. The microcomputer coordinates the inputs and outputs to all other components. PWM = pulse width modulation. pot = potentiometer value. LED = light-emitting diode.
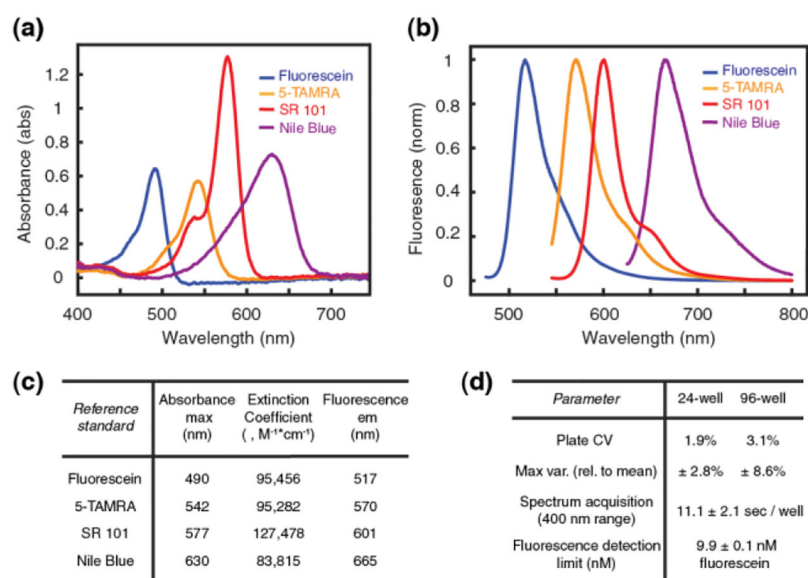
Figure 3. Characterization of the OSP using reference dyes.
Measurements were made according to commercial protocols (Thermo R14872). 5-TAMRA = 5-carboxytetramethyl-rhodamine; SR 101 = Sulforhodamine 101. **(a)** Absorbance spectra. **(b)** Fluorescence emission spectrum. **(c)** Key measured spectral parameters from a-b. **(d)** Key performance ranges. CV = Coefficient of variation across plate. Max var. = Variation range across plate. Spectrum acquisition time with 1.25 sec integration and includes stage motion to well. Detection limit error = stdev.
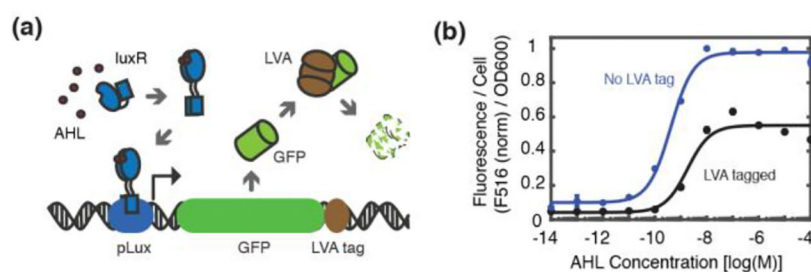
Figure 4. Cellular assays of a model of bacterial quorum sensing.
(a) Schematized genetic circuit of GFP expressed under the transcriptional regulation of the AHL ligand-inducible luxR transcriptional activator, and under the post-translational degradatory regulation of LVA protease. **(b)** Transfer function between the AHL input and GFP fluorescence output, with and without the LVA tag. Switching point values agree with previous reports [Ref 1]. F516 = Fluorescence at λ = 516nm, scaled to max. OD600 = Optical density at λ = 600nm. Error = s.e.m. (N=3).
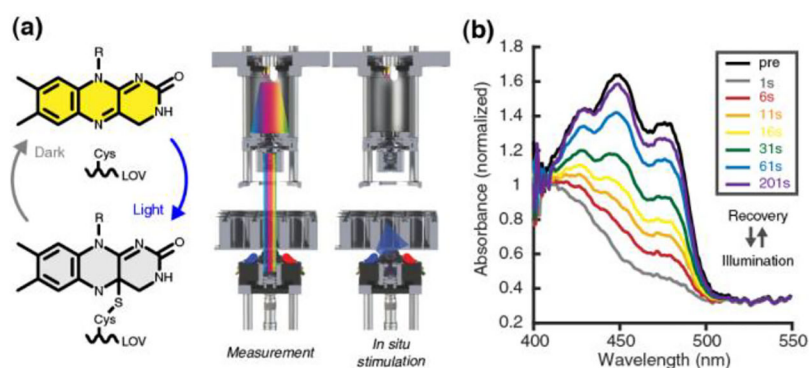
Figure 5. Flavin photocycling of EL222 by *in situ* optogenetic stimulation.
(a) Flavin photoadduct formation/reversion in a LOV sensor domain, measured by absorbance spectroscopy with *in situ* stimulation (λ = 470 nm @ 10 mW/cm2, 5 sec). **(b)** Representative flavin photocycling of 37 μM FPLC-purified recombinant holoprotein, normalized to its isobestic point. The triplet peak vibronic structure could be resolved, and the measured thermal reversion kinetics (τ = 31.5 sec, CI = ± 0.5 sec, N = 3; 5 sec sampling interval, measured at λ = 450nm) were in agreement with reported values. Pre = Pre-optogenetic stimulation, taken in the dark. Times = Post-illumination recovery in the dark.